

Packet Scheduling with Joint Design of MIMO and Network Coding

Miao Zhao and Yuanyuan Yang

Department of Electrical and Computer Engineering
State University of New York, Stony Brook, NY 11794, USA

Abstract— In this paper we propose a joint design of MIMO technique and network coding (MIMO-NC) and apply it to improve the performance of wireless networks. We consider a system in which the packet exchange among multiple wireless users is forwarded by a relay node. In order to enjoy the benefit of MIMO-NC, all the nodes in the network are mounted with two antennas and the relay node possess the coding capability. For the cross traffic flows among any four users, the relay node not only can receive packets simultaneously from two compatible users in the uplink (users-to-relay node), but also can mix up distinct packets for four destined users into two coded packets and concurrently send them out in the same downlink (relay node-to-users), so that the information content is significantly increased in each transmission. We formalize the problem of finding a schedule to forward the buffered data of all the users in minimum number of transmissions in such a system as a problem of finding a maximum matching in a graph. We also provide an analytical model on maximum throughput and optimal energy efficiency, which explicitly measures the performance gain of the MIMO-NC enhancement. Our analytical and simulation results demonstrate that system performance can be greatly improved by the efficient utilization of MIMO and network coding opportunities.

I. INTRODUCTION

Recent years have witnessed a great popularity and wide range of applications of wireless networks. In the meanwhile, the inherent characteristics of wireless networks, such as limited and shared medium, hostile interference and energy constraints, impose great challenges on improving system capacity [1].

One of the critical factors influencing the capacity of a wireless system is the radio technique. Recently, multiple-input multiple-output (MIMO) has been proposed as an effective radio technique to increase the data rate and provide reliable wireless communications. MIMO systems can offer *spatial multiplexing* gain and *spatial diversity* gain [1]. Spatial multiplexing creates extra dimensions in spatial domain, which can carry independent information in multiple data streams at the same time, thus greatly improves system capacity. Spatial multiplexing is also applicable to multiuser MIMO systems, namely, multiuser spatial multiplexing, which makes it possible for a user to simultaneously communicate with multiple users at high data rates [1], [3]. With the support of MIMO, if a relay node has two antennas, it can send/receive two packets to/from two users simultaneously whenever possible, therefore doubling the throughput in the ideal case. On the other hand, spatial diversity can be used to combat severe fading and improve reliability of wireless links by carrying duplicate copies of the same information along multiple antennas. MIMO technique

provides ample opportunities to improve the protocols and algorithms at the MAC layer and network layer.

Another emerging technique for improving system capacity is network coding [10]-[13]. Network coding was first studied for wireline networks in [6], which shows that by mixing the information in different messages at the nodes, a multicast can be performed at the same rate as that of a unicast from the sender to the receiver. Later it was shown in [7]-[9] that linear codes are sufficient to achieve the maximum capacity bounds for multicast traffic. In recent years, this promising technique has been extended to wireless networks [11]-[17]. By utilizing the characteristics of the broadcast channel, information in a wireless network is mixed and forwarded at intermediate relay nodes to improve network throughput and efficiency. The basic idea of network coding can be explained by a simple example consisting of three wireless nodes, where n_1 will send packet a to n_2 , while n_2 will send packet b to n_1 . Due to the limitation of the transmission range, the two packets have to be relayed by node R . In the standard packet forwarding, four transmissions are necessary to complete the end-to-end packet transfer. However, by using a simple form of network coding called XOR coding [11], the two packets can be transferred by only three wireless transmissions as follows: (1) n_1 transmits packet a to R ; (2) n_2 transmits packet b to R ; and (3) R transmits a new packet, c , obtained by performing an XOR coding on packets a and b . Due to the broadcast nature of the wireless channel, both n_1 and n_2 can receive the encoded packet and obtain each other's packet by decoding with their own packet. This leads to a coding gain of $4/3 = 1.3$.

We have seen that the aforementioned two approaches can potentially improve the system performance. Thus, an interesting question may arise: How much benefit can we achieve if we jointly consider the MIMO technique and network coding (for simplicity, we call it *MIMO-NC* in this paper)? MIMO-NC is feasibly implementable in wireless networks since it is not difficult to equip a node with two antennas and make it capable of coding. In fact, many wireless devices today have multiple antennas and embedded coding chips. In this paper, we study the joint design of MIMO-NC in a system in which a relay node takes the forwarding responsibility for the packet exchange among all the users. Such a system is typical and widely used in various wireless networks. It can be either a wireless local area network or a cluster component in a hierarchical wireless mesh network. Due to the complexity of MIMO and network coding, the motivation of this work is through exploiting such a simple system to gain some insights on MIMO-NC gains in general systems. Considering the cross traffic flows among any four users in such a system, each pair of two compatible users can simultaneously send data in an

Research supported by NSF grant numbers ECCS-0801438 and ECS-0427345 and ARO grant number W911NF-09-1-0154.

TABLE 1
TERMINOLOGIES

TERM	DEFINITION
Native Packet	A non-encoded packet.
Coded Packet	A packet that is XOR of two native packets.
Cross Traffic	Four unicast traffic flows (i.e., two pairs of flows) intersecting at relay node.
MIMO Gain	The ratio of the number of transmissions by the traditional SISO and non-coding approach, to the number of transmissions used by MIMO to deliver same set of packets.
Coding Gain	The ratio of the number of transmissions by the traditional SISO and non-coding approach to the number of transmissions used by network coding to deliver same set of packets.
MIMO-NC Gain	The ratio of the number of transmissions by the traditional SISO and non-coding approach to the number of transmissions used by MIMO-NC to deliver same set of packets.

uplink transmission, and the relay node can mix four received packets into two coded packets and send them in the same downlink transmission, such that more information content can be sent in each transmission. The idea of integrating MIMO into network coding has ever been mentioned in [18], which provides a decoding strategy that utilizes the redundancy produced by network coding schemes to achieve the spatial diversity gain. Such joint design is used to combat channel fading. In contrast, our work is quite different from it, which alternatively focuses on combining multiuser multiplexing with wireless network coding for packet forwarding so as to improve the system capacity and energy efficiency. We also study the optimal packet scheduling strategy with this joint design in the system with multiple users. We formalize the problem of sending out buffered packets of all the users in minimum time as a problem of finding a maximum matching in a graph. We then study the MIMO-NC performance by providing analytical bounds on maximum throughput and optimal energy efficiency. Packet scheduling with MIMO-NC requires the knowledge of different layers in the network, spanning from the states of the physical layer to the traffic patterns of the application layer, therefore, it is essentially a form of cross-layer design.

II. JOINT DESIGN OF MIMO AND NETWORK CODING

In this section, we present a novel packet forwarding scheme which utilizes the MIMO uplink and joint MIMO and network coding downlink to effectively increase the information content in each transmission. Before going into details, we refer readers to Table 1 for the terminologies to be used in the rest of the paper.

A. MIMO-NC Overview

Consider four users (denoted as n_1 to n_4) and a relay node (denoted as R) as shown in Fig. 1, where each node has two antennas and the relay node is capable of coding. The traffic among the users is unicast and is forwarded by the relay node, where n_1 and n_2 intend to exchange a pair of packets (a and b) via the relay node, and n_3 and n_4 intend to exchange another pair of packets (c and d). In the traditional approach, each packet is first sent to the relay node (i.e., uplink transmission),

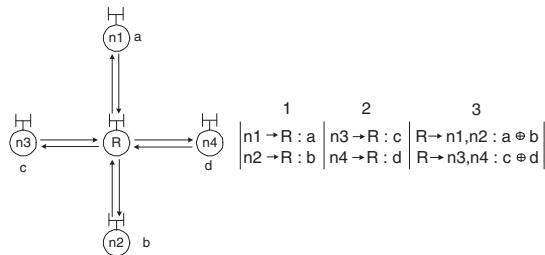


Fig. 1. Cross traffic flows and packet schedule with MIMO-NC in three transmissions.

and then forwarded to the destined user (i.e., downlink transmission). This process requires two transmissions to deliver a packet of a flow from its source to the destination. Thus, a total of eight transmissions are necessary to forward these four packets to their destinations. Now, consider the MIMO-NC approach, which utilizes spatial reuse and coding gain to increase the information content in each transmission. With two antennas, it is possible for a receiver to simultaneously receive distinct signals from two senders. Thus, it provides opportunities for two users to simultaneously transmit packets to the relay node in the uplink. In Fig. 1, we schedule n_1 and n_2 to concurrently send packet a and packet b to the relay node in one transmission, and then n_3 and n_4 to concurrently send packet c and packet d in another transmission. Thus four uplink transmissions are now reduced to two transmissions. Also note that with two antennas, a sender can send two distinct streams simultaneously. Once the relay node receives the four native packets, it XORs a and b , and c and d , respectively and sends the two coded packets ($a \oplus b$ for n_1 and n_2 , and $c \oplus d$ for n_3 and n_4) concurrently in one downlink transmission. Before sending out the two packets, the relay node adjusts the amplitude and phase of the transmitted signals on different antennas according to the channel state information such that the signals will add up constructively or destructively at each user as desired. Then, n_1 and n_2 can obtain each other's packets (b and a) by XORing $a \oplus b$ with their native packets. Similarly, n_3 and n_4 can finally obtain packet d and packet c . Four downlink transmissions are now completed in only one transmission. Thus, overall only three transmissions are required in MIMO-NC compared to eight transmissions in the traditional SISO and non-coding approach, which results in a MIMO-NC gain of $8/3 \approx 2.6$.

In fact, we have the freedom to mount more antennas on each node, which can support more concurrent information streams in one transmission and lead to higher MIMO-NC gain. However, it will likely become infeasible to mount a large number of antennas due to the constraint on the distances among antennas to ensure independent fading. Thus, we only consider the case of two antennas for each node in the system. Moreover, it is intuitive that more flows may be encoded together when there are more than four users in the system such that the downlink transmissions can be dramatically reduced. However, this would require each user to constantly overhear packets on the channel and locally maintain the information that is temporarily or permanently useless. Otherwise, they may not be able to successfully decode the received coded packets with local information. To keep the structure of MIMO-NC simple, we do not consider such opportunistic listening [11] and only consider encoding two independent native packets in

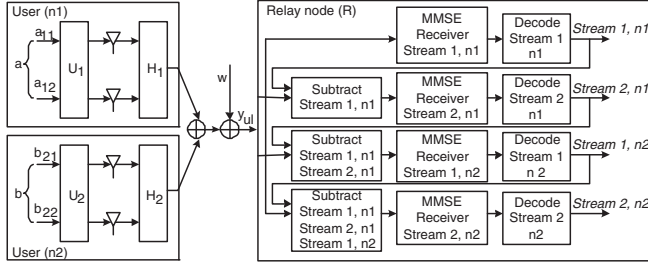


Fig. 2. Transceiver strategy for the two-user MIMO uplink: two users simultaneously transmit packets to the relay node.

this paper.

To see how beneficial MIMO-NC could be, let's compare its performance with the cases where only MIMO technique or network coding is used. First, consider an approach that utilizes only MIMO technique for the cross traffic among four users, in which two compatible users simultaneously communicate with the relay node in both uplink and downlink with the support of multiuser spatial multiplexing and uplink-downlink duality. The following is a possible sequence of transmissions: (1) n_1 and n_2 send packet a and packet b to the relay node simultaneously; (2) n_3 and n_4 send packet c and packet d to the relay node simultaneously; (3) the relay node concurrently sends packet a to n_2 and packet b to n_1 ; and (4) the relay node concurrently sends packet c to n_4 and packet d to n_3 . In this case, the information content in each transmission is doubled, resulting in a MIMO gain of 2. Next, consider the approach that only utilizes network coding. If we do not consider the opportunistic listening among the users, the coding gain is still 1.3 for the cross traffic as mentioned in Section I. In contrast, the MIMO-NC gain for the cross traffic among four users is approximately 2.6 as discussed above, which clearly outperforms other schemes. Next, we discuss the underlying design principles and the transceiver architecture of MIMO-NC in detail.

B. MIMO Uplink

In this subsection, we look into the role of two transmit antennas at each user and two receive antennas at the relay node, which enable the two users to send their native packets to the relay node simultaneously such that MIMO capacity can be achieved in the uplink.

The uplink transmitter and receiver architecture are illustrated in Fig. 2 [1][2]. Suppose n_1 and n_2 are transmitters that intend to transmit packet a and packet b simultaneously to the relay node. Each of them splits its native data and encodes them into two independent streams of information, i.e., packet a is divided into a_{11} and a_{12} while packet b is divided into b_{21} and b_{22} . Powers P_{k1} and P_{k2} ($k = 1, 2$) are allocated to the two streams of user n_k , passed through a rotation \mathbf{U}_k and sent over the antenna array at user n_k . The 2×2 rotation \mathbf{U}_k is chosen to correspond to the right rotation in the singular value decomposition (SVD) of channel matrix \mathbf{H}_k and the power allocated to the data streams corresponds to the waterfilling allocations over the squared singular values of \mathbf{H}_k . The two-user MIMO uplink transmission can be modeled as

$$\mathbf{y}_{ul} = \mathbf{H}_1 \mathbf{U}_1 \mathbf{a} + \mathbf{H}_2 \mathbf{U}_2 \mathbf{b} + \mathbf{w} \quad (1)$$

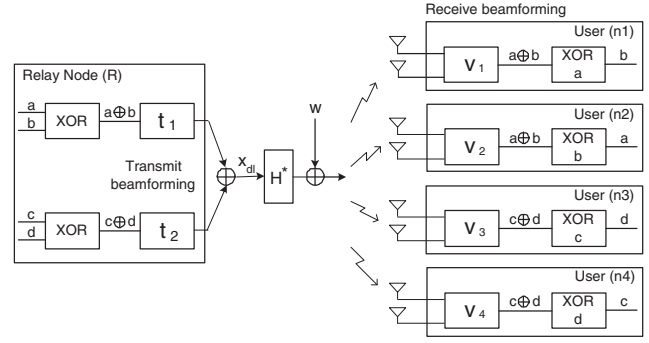


Fig. 3. Transceiver strategy for the MIMO downlink with network coding.

where $\mathbf{a} = [a_{11}, a_{12}]^T$, $\mathbf{b} = [b_{21}, b_{22}]^T$, \mathbf{y}_{ul} is the received signal vector at the relay node, \mathbf{H}_k is a 2×2 channel matrix between n_k and the relay node, and \mathbf{w} is the i.i.d. $\mathcal{CN}(0, \sigma^2 \mathbf{I}_2)$ background Gaussian noise. The relay node uses the minimum mean square error receiver with successive interference cancellation (MMSE-SIC) to decode the data streams of two distinct users. The MMSE receiver is the optimal compromise between maximizing the signal strength from the user of interest and suppressing the interference from the other user. n_1 's data is first decoded and the corresponding two transmit data streams are subtracted off. The output SINR of the MMSE receiver for n_1 would treat n_2 's signal as colored Gaussian interference, while n_2 only has to contend with the background Gaussian noise and ensure its performance to meet the single-user bound. By choosing a different cancellation order, the users are prioritized differently in sharing the common resource of the uplink channel, in the sense that the user canceled later is treated better [1]. Explicitly, the rates of n_1 and n_2 , R_1 and R_2 , achieved by this transceiver architecture can be expressed as

$$\begin{aligned} R_1 &= \log \det [\mathbf{I}_2 + \mathbf{H}_1 \mathbf{U}_1 \mathbf{\Lambda}_1 (\sigma^2 \mathbf{I}_2 + \mathbf{H}_2 \mathbf{U}_2 \mathbf{\Lambda}_2 \mathbf{U}_2^* \mathbf{H}_2^*)^{-1} \mathbf{U}_1^* \mathbf{H}_1^*] \\ R_2 &= \log \det (\mathbf{I}_2 + \frac{1}{\sigma^2} \mathbf{H}_2 \mathbf{U}_2 \mathbf{\Lambda}_2 \mathbf{U}_2^* \mathbf{H}_2^*) \end{aligned} \quad (2)$$

where $\mathbf{\Lambda}_k$ ($k = 1, 2$) is a diagonal matrix with two diagonal entries equal to the power allocated to data streams (P_{k1} , P_{k2}) of n_k .

In general, different choices of power splits and rotations lead to different achievable MIMO capacity. Depending on the performance tradeoff between two users in the uplink, different input strategies may be adopted. Since the total transmitted power of each user is limited and the input strategy may result in a lower SINR of the received signals than the receive sensitivity of the relay node, not all pairs of users can successfully make concurrent packet transmissions in the uplink. If any two users can work together in the uplink transmission, we say these two users or their packets are *uplink-compatible*. In the case where two users are uplink-incompatible, they have to send packets to the relay node one by one as in the traditional SISO approach.

C. MIMO Downlink with Network Coding

In this subsection, we study how the downlink is affected by the availability of two transmit antennas at the relay node and two receive antennas at each user, and its incorporation with network coding.

The downlink transceiver architecture is illustrated in Fig. 3. The relay node XORs the received four packets into two coded packets ($a \oplus b$ and $c \oplus d$). It intends to send packet $a \oplus b$ to n_1 and n_2 , and send packet $c \oplus d$ to n_3 and n_4 . Suppose P_1 and P_2 are the transmit powers allocated for the two coded packets with a total power constraint P . The transmitted signals at the antenna array of the relay node can be expressed as

$$\mathbf{x}_{dl} = \mathbf{t}_1(a \oplus b) + \mathbf{t}_2(c \oplus d) \quad (3)$$

where \mathbf{t}_1 and \mathbf{t}_2 are transmit filters for the two coded packets. If we apply filter \mathbf{v}_k for receive beamforming at user n_k , the SINR of the received signal at each user is given by

$$\begin{aligned} \text{SINR}_k^{dl} &= \frac{P_1 \|\mathbf{v}_k^* \mathbf{H}_k \mathbf{t}_1\|^2}{\sigma^2 + P_2 \|\mathbf{v}_k^* \mathbf{H}_k \mathbf{t}_2\|^2}, \quad k = 1, 2 \\ \text{SINR}_k^{dl} &= \frac{P_2 \|\mathbf{v}_k^* \mathbf{H}_k \mathbf{t}_2\|^2}{\sigma^2 + P_1 \|\mathbf{v}_k^* \mathbf{H}_k \mathbf{t}_1\|^2}, \quad k = 3, 4 \end{aligned} \quad (4)$$

Note that receive filter \mathbf{v}_k for the particular received signal of n_k does not affect the SINR of other users' signals. Therefore, the optimal receive filters can be found to maximize each of the SINRs of the four users with respect to the given transmit filters \mathbf{t}_1 and \mathbf{t}_2 . However, since the SINR of each user is a function of both transmit filters \mathbf{t}_1 and \mathbf{t}_2 , transmit filters cannot be optimized independently. Therefore, similar to [5], we use the product of SINR as a performance metric of the system capacity. \mathbf{t}_1 and \mathbf{t}_2 are correspondingly chosen to maximize the SINR product of the four users. As a result, the selection of the filters at the relay node and users can be written as

$$(\mathbf{t}_m, \mathbf{v}_k)_{opt} = \arg \max_{\mathbf{t}_m, \mathbf{v}_k, \|\mathbf{t}_m\|^2 = \|\mathbf{v}_k\|^2 = 1} \prod_{k=1}^4 \text{SINR}_k^{dl} \quad (5)$$

for $m = 1, 2$ and $k = 1, 2, 3, 4$.

In the case where $\|\mathbf{H}_1\|$ and $\|\mathbf{H}_2\|$ are significantly different from $\|\mathbf{H}_3\|$ and $\|\mathbf{H}_4\|$ (assuming $\|\mathbf{H}_1\|, \|\mathbf{H}_2\| \leq \|\mathbf{H}_3\|, \|\mathbf{H}_4\|$), we can perform the superposition coding with successive interference cancellation as follows: The transmit signal is the linear superposition of the two coded packets ($a \oplus b$ and $c \oplus d$). Then, n_1 and n_2 would decode packet $a \oplus b$ and treat the part of packet $c \oplus d$ in their received signals as noise. Finally, n_3 and n_4 which have better SINR first decode packet $a \oplus b$, subtract it from their received signals and then decode packet $c \oplus d$, which is the packet they are interested in. With a total power constraint P and splitting this among the two coded packets $P = P_1 + P_2$, we can write the rate for n_k that is achieved with the receiver architecture in Fig. 3 and superposition coding as

$$\begin{aligned} R_1 &= \log \left(1 + \frac{P_1 \|\mathbf{v}_1^* \mathbf{H}_1 \mathbf{t}_1\|^2}{\sigma^2 + P_2 \|\mathbf{v}_1^* \mathbf{H}_1 \mathbf{t}_2\|^2} \right), \quad R_2 = \log \left(1 + \frac{P_1 \|\mathbf{v}_2^* \mathbf{H}_2 \mathbf{t}_1\|^2}{\sigma^2 + P_2 \|\mathbf{v}_2^* \mathbf{H}_2 \mathbf{t}_2\|^2} \right) \\ R_3 &= \log \left(1 + \frac{P_2 \|\mathbf{v}_3^* \mathbf{H}_3 \mathbf{t}_2\|^2}{\sigma^2} \right), \quad R_4 = \log \left(1 + \frac{P_2 \|\mathbf{v}_4^* \mathbf{H}_4 \mathbf{t}_2\|^2}{\sigma^2} \right) \end{aligned} \quad (6)$$

Assume each user still has a copy of its native packet. Once n_1 successfully receives packet $a \oplus b$, it can obtain packet b by XORing packet $a \oplus b$ with packet a . Similarly, n_2, n_3 and n_4 can obtain packets a, d and c , respectively. Thus the four downlink transmissions required by the traditional SISO and non-coding approach now can be done in only one downlink transmission with the support of MIMO-NC. Note that different transceiver strategies result in different achievable downlink performance among users. Even for the same transceiver, different choices of power allocation and filters

lead to different downlink capacity. Similar to the situation in the uplink, the setting of these parameters is based on how to balance the priorities among users in the downlink. If the four users can successfully decode their interested packets in the same transmission, we say the two coded packets or the two pairs of flows are *downlink-compatible*. In the case where packet $a \oplus b$ and packet $c \oplus d$ are downlink-incompatible, they need to be transmitted separately in the following transmission sequence: (1) If packet a and packet b are uplink-compatible, the relay node can send packet a to n_2 and packet b to n_1 simultaneously in a transmission due to the uplink-downlink duality [1], otherwise, the relay node can only transmit them one by one as in the traditional SISO approach; (2) Similarly, the relay node can send packet c to n_4 and packet d to n_3 simultaneously in one downlink transmission if they are uplink-compatible, otherwise, the relay node will send them one by one. Therefore, at least two downlink transmissions are required.

III. OPTIMAL SCHEDULE FOR RELAY NODE WITH MIMO-NC

In the previous section, we discussed the working principle of MIMO-NC. We now consider the scheduling of the relay node when adopting MIMO-NC with multiple users (may be more than 4 users) in the system.

Since the objective of the scheduling is to send out the packets in all the users as soon as possible, clearly, in an optimal schedule the relay node should try to match two uplink-compatible packets for uplink transmission or match two downlink-compatible pairs of packets for downlink transmission as much as possible. In other words, any four packets from different users are desired to be grouped together to utilize the MIMO-NC whenever possible. Thus the problem of finding an optimal schedule is equivalent to finding a maximum number of such 4-member groups among the packets based on their compatibility relationship. In practice, each user may have many packets to be exchanged with others. As a result, the sizes of the compatibility matrices among packets can be quite large. Fortunately, the sizes can be reduced by taking advantage of the fact that when two users are compatible, each packet of a user will be compatible with all the packets of the other. Thus, if we consider the steady state of traffic flows which assumes that the same number of packet pairs are to be exchanged for each link, finding 4-member groups among packets can be reduced to finding such groups among the users. Without loss of generality, we simply assume that a pair of packets is to be exchanged between any two intended users in the following discussion.

We now use an example in Fig. 4 to explain the basic principle of our approach. Give a system with five users denoted by n_1 to n_5 and the relay node is not shown in the figure. Each packet needs to be forwarded by the relay node. The traffic pattern among the users is given in a symmetric matrix \mathbf{L} , where an entry $l_{ij} = 1$ if the corresponding users i and j have a pair of packets to be exchanged, otherwise is 0. The uplink-compatibility relationship between any two users and the downlink-compatibility relationship between any two pairs of packets to be exchanged are given in the symmetric matrices \mathbf{C}^{ul} and \mathbf{C}^{dl} , respectively, with each entry set to 1 if

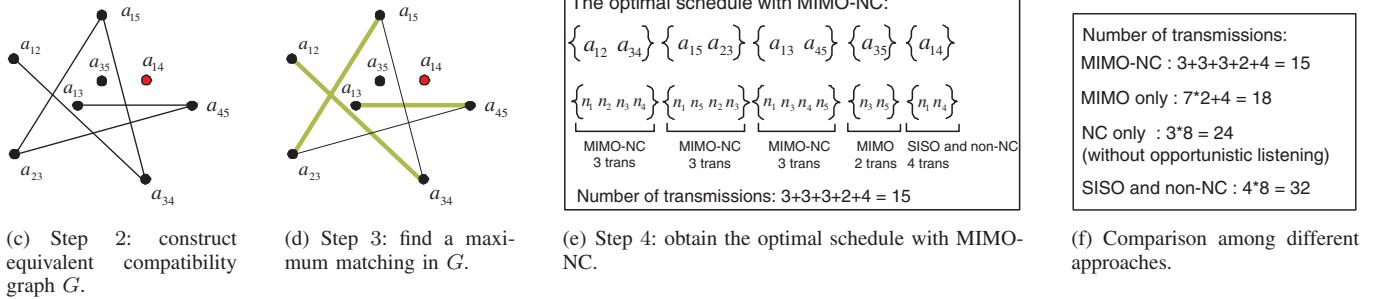
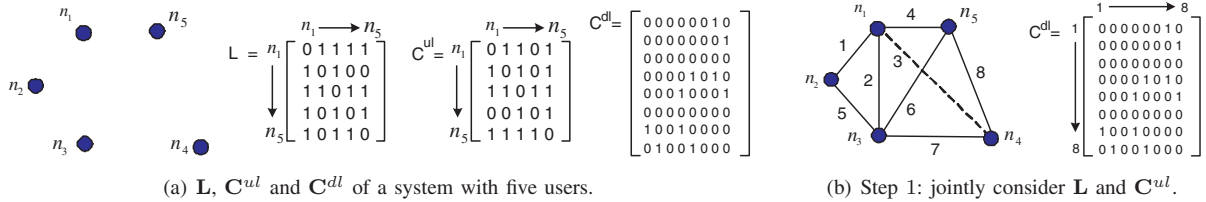


Fig. 4. Illustration of optimal schedule for the relay node.

they are compatible. C^{ul} and C^{dl} are maintained by the relay node with the results of periodical channel estimations. All the information in the example is shown in Fig. 4(a).

In the first step, we jointly consider the traffic pattern and the uplink compatibility relationship among the users. In particular, if $l_{ij} = 1$, user n_i and user n_j ($i < j$) are connected by a solid link when n_i and n_j are uplink-compatible (i.e., $c_{ij}^{ul} = 1$ in C^{ul}), or by a dashed link when n_i and n_j are uplink-incompatible (i.e., $c_{ij}^{ul} = 0$ in C^{ul}). Based on the information in Fig. 4(a), the scenario after the first step is depicted in Fig. 4(b), where there are a total of eight links, seven out of which are solid links and the remaining one is a dashed link. Each link represents a pair of packets to be exchanged between two intended users and we call the two links that share no common user the *disjoint links*.

Since we intend to group four users each time to exchange two pairs of packets by MIMO-NC, which is equivalent to scheduling the solid links in pairs, we need to take downlink compatibility among the links into consideration. In the second step, with the further consideration on downlink compatibility, we formalize the system as a graph called *equivalent compatibility graph* and denote it as G . Each link between n_i and n_j corresponds to a vertex a_{ij} in G . There is an edge $(a_{ij}, a_{i'j'})$ in G between vertices a_{ij} and $a_{i'j'}$ when the corresponding links are two disjoint solid links and downlink-compatible with each other. This also implies that the dashed links in the system will become isolated vertices in G . Fig. 4(c) shows an example of the equivalent compatibility graph constructed based on the system in Fig. 4(b) with the information of C^{dl} . The dashed link between n_1 and n_4 in Fig. 4(b) corresponds to an isolated vertex, a_{14} , in G as plotted in Fig. 4(c). We call such a vertex a *fully-isolated vertex* since n_1 and n_4 are incompatible in the uplink and the link between them is also downlink-incompatible with all other links. Thus, four transmissions are necessary to exchange a pair of packets between n_1 and n_4 . The solid link between n_3 and n_5 in Fig. 4(b) labeled as link 6 shares a common user with all other solid links, except the link between n_1 and n_2 labeled as link 1. However, $c_{16}^{dl} \in C^{dl}$ is equal to 0, which indicates that these two links are downlink-

incompatible. Thus, the link between n_3 and n_5 corresponds to another type of isolated vertex, a_{35} , in G . We call such a vertex a *half-isolated vertex* since though the two users (i.e., n_3 and n_5) are uplink-compatible to each other, the link between them is downlink-incompatible with all its disjoint solid links. Then a pair of packets to be exchanged between these two users needs two transmissions by utilizing uplink-downlink duality [1]. Other vertices in G are non-isolated vertices, and each of them corresponds to a solid link which is downlink-compatible with some of other disjoint solid links. For example, the solid link between n_1 and n_5 in Fig. 4(b) labeled as link 4 is disjoint with two other solid links (link 5 between n_2 and n_3 and link 7 between n_3 and n_4), and is downlink-compatible with both of them (i.e., $c_{45}^{dl} = 1$ and $c_{47}^{dl} = 1$). Hence, link 4 between n_1 and n_5 is abstracted as a non-isolated vertex a_{15} in G which is adjacent to a_{23} and a_{34} . The reason why only two disjoint solid links are qualified to be adjacent in an equivalent compatibility graph is because that it is not desirable to let a user be the destination of the two encoded packets simultaneously in the same downlink transmission.

When two adjacent non-isolated vertices in G are matched into a pair, it is equivalent to grouping four users together to exchange two pairs of packets among them, which can be efficiently done in three transmissions with the support of MIMO-NC. Thus, the problem of finding 4-member groups is simplified to the problem of finding a matching among the vertices in G . Therefore, the third step of finding an optimal schedule is reduced to finding a maximum matching in G . Fig. 4(d) provides the maximum matching found in G for the example denoted by the bold edges. We can see that besides two isolated vertices a_{14} and a_{35} , other vertices in G can be matched into three pairs to the maximum extent.

Now the last step is to construct the optimal schedule based on the maximum matching in G . The optimal schedule for the example is listed in Fig. 4(e). For each matching edge in G , the corresponding 4 users are grouped together to utilize MIMO-NC, in which two pairs of packets are exchanged in three transmissions. For each half-isolated or full-isolated vertex in G , the packet exchange between the corresponding

two users requires two and four transmissions, respectively. Thus, in the example, 16 packets would be forwarded to their destinations in 15 transmissions with MIMO-NC, achieving a MIMO-NC gain of 2.13 compared to 32 transmissions in the traditional SISO and non-coding approach. Consider utilizing only MIMO technique in the scenario of Fig. 4(b). As discussed earlier, two transmissions are required for each solid link and four transmissions are necessary for each dashed link in the system. Therefore, a total of 18 transmissions are needed, which leads to a MIMO gain of 1.78. If we apply only network coding in the example, three transmissions are necessary in the absence of opportunistic listening for each link in Fig. 4(b). Thus, eight pairs of packet exchange can be completed in 24 transmissions, producing a coding gain of 1.33. The comparison on the number of required transmissions among different approaches is listed in Fig. 4(f). Clearly, MIMO-NC significantly outperforms other approaches due to the increase of the information content carried in each transmission, which leads to higher utilization of network resource.

In summary, the basic idea of finding an optimal schedule with MIMO-NC for the relay node is to construct an equivalent compatibility graph and find a maximum matching in it. Note that this approach can be applied to a system with any number of users, general traffic pattern and compatibility relationship.

In general, maximum matching in a graph can be found in polynomial time by algorithms such as Edmonds' Blossom algorithm [20][19] which takes $O(|V|^3)$ time, where $|V|$ is the number of vertices in the graph. In our case, there are K users, with each user intending to exchange packets with all the other users. Thus there would be $\frac{1}{2}K(K-1)$ vertices in G in the worst case, and it would take $O(K^6)$ time to find a maximum matching in G . For the applications with a large number of users, we can also consider using a fast approximate algorithm which is capable of finding a fairly good matching in a graph. The simplest and most well-known approximation algorithm is to simply return a maximal matching [20], which has $O(|E|)$ time complexity, where $|E|$ is the number of edges in the graph, and has a performance ratio of 1/2, which means that the matching found has a size at least half of the maximum matching. Recently, a simple $O(|E|)$ approximation algorithm for maximum matching was given in [4] with an improved performance ratio of 3/4. Thus, in the worst case, it would take $O(K^4)$ time to find a matching in G with 3/4 performance ratio by this algorithm.

IV. PERFORMANCE STUDY

Having discussed the optimal schedule for the relay node, in this section, we study the system performance after enhanced with MIMO-NC by an analytical model and simulations.

Intuitively, the benefit of MIMO-NC depends on the opportunities of utilizing network coding and MIMO technique. Coding opportunities are determined by the traffic pattern and the listening mechanism. In the scenario we consider, packets are always exchanged between two users and forwarded by a relay node. This is a typical scenario in wireless networks and provides ample opportunities to utilize network coding. MIMO opportunity depends on many factors, such as the physical environment, power allocation, and transceiver strategies. Thus, the performance evaluation of MIMO-NC in general is a

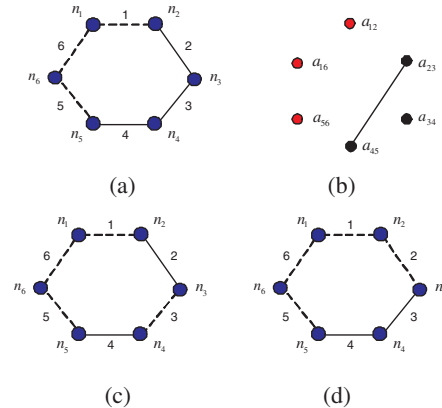


Fig. 5. Circular traffic patterns with $K = 6$. (a) An example of circular traffic pattern among 6 users with 3 solid links and 3 dashed links; (b) Equivalent compatibility graph G of the system in (a); (c) $K - 2$ dashed links, among which $K - 3$ links are consecutively connected; (d) $K - 2$ dashed links which are consecutively connected.

difficult task. Fortunately, we can use the uplink compatibility probability between two users and the downlink compatibility probability between two pairs of flows to describe the MIMO-NC opportunities, since these probabilities are generally steady in a static topology or a similar environment such as wireless LANs and mesh networks.

A. An Analytical Model on Maximum Throughput and Optimal Energy Efficiency

In this subsection, we give an analytical model which characterizes the maximum throughput and optimal energy efficiency of the system enhanced by MIMO-NC. For clarity, we consider the normalized throughput and normalized energy efficiency. The *normalized throughput* λ is defined as the number of packets divided by the number of transmissions required to forward these packets to their destinations, while the *normalized energy efficiency* ζ is defined as the total energy consumption divided by the number of transmitted packets.

Consider a relay node and a total of K users, denoted by n_1, n_2, \dots, n_K . Each packet needs to be forwarded by the relay node. In the traditional SISO and non-coding approach, clearly, regardless of the number of users and the traffic pattern among them, we have $\lambda_{max} = 0.5$ pkts/tran since the end-to-end delivery of each packet always needs two transmissions, where λ_{max} denotes the maximum throughput without considering the communication overhead in the MAC layer. Assume that the power consumption for a radio of each user in sensing, receiving and transmitting states during each transmission is W_s , W_r and W_t , respectively. Then the optimal energy efficiency for the traditional SISO and non-coding approach is given by

$$\zeta_{opt} = 2 [W_t + W_r + (K - 1)W_s] \quad (7)$$

Next, we derive λ_{max} and ζ_{opt} when MIMO-NC is adopted.

1) MIMO-NC Performance with Circular Traffic Pattern:

To facilitate the analysis, we firstly consider the MIMO-NC performance with a basic and typical traffic pattern called *circular traffic pattern*, in which user n_i has packets to exchange with users n_{i-1} and n_{i+1} for $1 < i < K$, n_1 has packets to exchange with n_2 and n_K , and n_K has packets to exchange with n_{K-1} and n_1 . Through analyzing this traffic pattern, we

would like to obtain some insights into the factors that affect the MIMO-NC gain. We will extend the performance analysis to the case with general traffic pattern in the next subsection.

In the circular traffic pattern, there are K links in the system, each representing a pair of flows to be exchanged between two users. It also means that there are K vertices in the equivalent compatibility graph G . Fig. 5(a) gives an example of the circular traffic pattern among six users, where there are three solid links and three dashed links. We denote the uplink compatibility probability between any two users as p_1 and the downlink compatibility probability between any two links as p_2 . As mentioned earlier, the link associated with two uplink-incompatible users is not qualified to be downlink compatible with other links. Thus, considering the importance of p_1 and trying to keep our analysis clear and tractable, we simply assume that $p_2 = 1$ in this case, which means that any two disjoint solid links are always downlink-compatible with each other.

Suppose among the K vertices in G , c vertices are non-isolated and the remaining $K - c$ vertices are isolated. The optimal schedule which aims to forward packets in the fastest way is equivalent to always matching the non-isolated vertices of G into pairs. In other words, c non-isolated vertices can be matched into at most $c/2$ pairs, which leads to the minimum number of transmissions. We assume that the relay node can switch its operation only between MIMO-NC and the traditional SISO and non-coding approach. This means that any two paired non-isolated vertices in G correspond to three transmissions for exchanging two pairs of packets by the MIMO-NC among the users in the corresponding 4-member group. In contrast, each isolated vertex a_{ij} in G , either half-isolated or fully-isolated, corresponds to four transmissions for exchanging a pair of packets between users n_i and n_j . Thus, the maximum throughput and the optimal energy efficiency can be given by

$$\lambda_{max} = \frac{2K}{3 \cdot \frac{c}{2} + 4(K-c)} = \left(2 - \frac{5c}{4K}\right)^{-1} \quad (8)$$

$$\zeta_{opt} = \frac{\frac{c}{2}[5W_t + 6W_r + (3K-1)W_s] + 4(K-c)[W_t + W_r + (K-1)W_s]}{(2 - \frac{3c}{4K})W_t + (2 - \frac{c}{2K})W_r + (2K - \frac{5}{4}c - 2 - \frac{3c}{4K})W_s} \quad (9)$$

The number of non-isolated vertices c is a random variable. Let $P_K(l)$ be the probability that out of K vertices in G , there are l isolated vertices. The average maximum throughput and average optimal energy efficiency can be written as

$$\begin{aligned} \bar{\lambda}_{max} &= \sum_{c=0}^K P_K(K-c) \cdot \lambda_{max}, \\ \bar{\zeta}_{opt} &= \sum_{c=0}^K P_K(K-c) \cdot \zeta_{opt} \end{aligned} \quad (10)$$

To find $P_K(l)$, let condition on the number of dashed links in the system. Let E_i be the event that among K links, there are i dashed links, the probability of which is denoted as $P_e(i)$. Let L be the random variable denoting the number of isolated vertices in G . $P_K(l)$ can be expressed as

$$P_K(l) = P(L=l) = \sum_{i=0}^K P_e(i) P_K(L=l|E_i) \quad (11)$$

Recall that the isolated vertices are formed in G due to two reasons: (1) the dashed links in the system are abstracted to fully-isolated vertices in G , e.g., vertices a_{12} , a_{16} and a_{56} in

Fig. 5(b); (2) the solid links, whose disjoint links are all dashed links or being downlink-incompatible with all the disjoint solid links, correspond to half-isolated vertices in G . Since we assume that a solid link is always downlink-compatible with its disjoint solid links, the only way a half-isolated vertex a_{ij} is formed in G due to reason (2) is that the disjoint links of the link between n_i and n_j are all dashed links, e.g., vertex a_{34} in Fig. 5(b). Clearly, if there are i dashed links, there are at least i isolated vertices in G . Therefore, for $i > l$, $P_K(L=l|E_i) = 0$. In the circular traffic case we consider, each link has exactly $K-3$ disjoint links, which are consecutively connected. For the example shown in Fig. 5(a), link 1 is disjoint with three links, which are links 3, 4 and 5. Next, we will derive $P_K(l)$ separately in different cases.

Case 1: $l < K-3$. Since $i \leq l$, the possible number of dashed links is also less than $K-3$. Under this condition, the disjoint links of a solid link could not all be dashed links due to the fact that it has $K-3$ disjoint links. All the isolated vertices in G are fully-isolated vertices due to reason (1), which means that there could be only l dashed links in the system, i.e., $P_K(L=l|E_i) = 0$ for any $i < l$ and $P_K(L=l|E_l)=1$. Thus $P_K(l)$ can be rewritten as

$$\begin{aligned} P_K(l) &= \sum_{i=0}^l P_e(i) P_K(L=l|E_i) = P_e(l) P_K(L=l|E_l) \\ &= \binom{K}{l} (1-p_1)^l p_1^{K-l} \quad (l < K-3) \end{aligned}$$

Case 2: $l = K-3$. As discussed in Case 1, if $i < K-3$, there is no possibility to produce $K-3$ isolated vertices in G , i.e., $P_K(L=K-3|E_i) = 0$ for any $i < K-3$. Thus, there should be $K-3$ dashed links. Note that these $K-3$ dashed links cannot be consecutive, otherwise, it will produce an extra half-isolated vertex in G due to reason (2). Now, $P_K(l)$ can be given by

$$\begin{aligned} P_K(l) &= P_K(K-3) = \sum_{i=0}^{K-3} P_e(i) P_K(L=K-3|E_i) \\ &= P_e(K-3) [1 - P_K(L=K-2|E_{K-3})] \\ &= \binom{K}{K-3} (1-p_1)^{K-3} p_1^3 \left[1 - \frac{K}{\binom{K}{K-3}} \right] \end{aligned}$$

Case 3: $l = K-2$. Again, $P_K(L=K-2|E_i) = 0$ for any $i < K-3$. There are two scenarios that lead to $K-2$ isolated vertices in G : (1) There are $K-3$ dashed links, which are consecutively connected. These $K-3$ dashed links correspond to the $K-3$ fully-isolated vertices in G and the consecutive connections among them lead to an extra half-isolated vertex in G . (2) There are $K-2$ dashed links, which cannot incur any extra half-isolated vertex in G . Since $K-3$ consecutive dashed links may cause an extra half-isolated vertex in G , let us consider two sub-cases of the second scenario. The first sub-case is that, among $K-2$ dashed links in the system, there are $K-3$ consecutive dashed links and the last link is disjoint with these $K-3$ consecutive dashed links. Fig. 5(c) shows an example in this situation. Note that links 1, 6 and 5 are three consecutive dashed links, which are all the disjoint links of link 3. Clearly, this sub-case will not incur any extra half-isolated vertex in G . The second sub-case is that all these $K-2$ dashed links are consecutively connected. An example of this case is shown in Fig. 5(d). The disjoint links of link 3 and link 4 are all dashed ones. Consequently, link 3 and link

4 will be abstracted to two extra half-isolated vertices in G . Thus, if $K - 2$ dashed links are all consecutively connected, it will result in K isolated vertices in G , otherwise, only $K - 2$ fully-isolated vertices exist in G . As a result, $P_K(l)$ can be rewritten as

$$\begin{aligned}
P_K(K-2) &= P_e(K-3)P_K(L=K-2|E_{K-3}) \\
&\quad + P_e(K-2)P_K(L=K-2|E_{K-2}) \\
&= P_e(K-3)P_K(L=K-2|E_{K-3}) \\
&\quad + P_e(K-2) \cdot [1 - P_K(L=K|E_{K-2})] \\
&= \binom{K}{K-3} (1-p_1)^{K-3} p_1^3 \left[\frac{\frac{K}{K-3}}{\binom{K}{K-3}} \right] \\
&\quad + \binom{K}{K-2} (1-p_1)^{K-2} p_1^2 \left[1 - \frac{\frac{K}{K-2}}{\binom{K}{K-2}} \right]
\end{aligned}$$

Case 4: $l = K - 1$. Apparently, this case could not occur since it is impossible that there is only one non-isolated vertex in G . Thus $P_K(K - 1) = 0$.

Case 5: $l = K$. Clearly, $P_K(L = K|E_i) = 0$ for any $i \leq K - 3$. There are three scenarios that result in K isolated vertices in G : (1) $i = K - 2$. As discussed in Case 3, $K - 2$ dashed links should be consecutively connected. (2) $i = K - 1$. Since the disjoint links of the only solid link are all dashed links, it will incur an extra half-isolated vertex in G , resulting in a total of K isolated vertices in G . Thus, $P_K(L = K|E_{K-1}) = 1$. (3) $i = K$. In this case, K dashed links in the system correspond to K isolated vertices in G , i.e., $P_K(L = K|E_K) = 1$.

$$\begin{aligned}
P_K(K) &= P_e(K-2)P_K(L=K|E_{K-2}) + \\
&\quad P_e(K-1)P_K(L=K|E_{K-1}) + \\
&\quad P_e(K)P_K(L=K|E_K) \\
&= \binom{K}{K-2} (1-p_1)^{K-2} p_1^2 \left[\frac{\frac{K}{K-2}}{\binom{K}{K-2}} \right] + \\
&\quad K(1-p_1)^{K-1} p_1 + (1-p_1)^K
\end{aligned}$$

Fig. 6 shows the average maximum throughput and average optimal energy efficiency of MIMO-NC with the circular traffic pattern under different uplink compatibility probabilities p_1 . We can see that a significant improvement can be achieved when the compatibility probability between two users increases. For example, when $K = 10$ and $p_1 = 0.5$, the average maximum throughput of MIMO-NC is 0.74 pkts/tran as shown in Fig. 6(a), which is a 48% increase compared to that of the traditional SISO and non-coding approach. Here we assume that W_t , W_r and W_s are of 2, 1.5 and 1 energy units, respectively. In fact, since we are only interested in how MIMO-NC enhances the channel utilization to save energy, not the exact amount of energy consumption, this assumption has little impact on the conclusions drawn. When $K = 10$ and $p_1 = 0.5$, the optimal energy efficiency is 17.31 energy_units/pkt as shown in Fig. 6(b). It results in 31% improvement compared with that of the traditional SISO and non-coding approach, whose energy efficiency is 25 energy_units/pkt.

2) MIMO-NC Performance with General Traffic Pattern:

We now extend the analysis to the general case. In order to describe the general traffic pattern in the system, we introduce traffic probability p , with which there is a pair of flows to be exchanged between any two users. Apparently, the probability

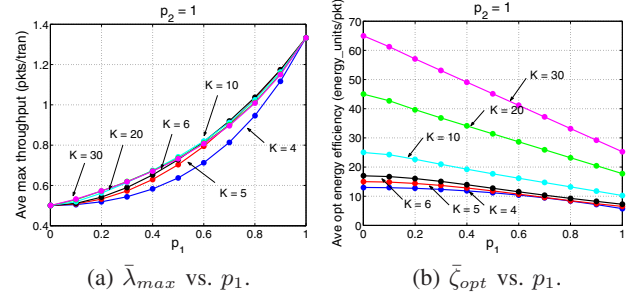


Fig. 6. Average maximum throughput and average optimal energy efficiency of MIMO-NC with circular traffic pattern as functions of p_1 .

that there exist N links in the system with a total of K users can be written as

$$P_K(N) = \binom{\frac{1}{2}K(K-1)}{N} \cdot p^N \cdot (1-p)^{\frac{1}{2}K(K-1)-N} \quad (12)$$

Clearly, in the traditional SISO and non-coding approach, the average maximum throughput and average optimal energy efficiency are given by

$$\begin{aligned}
\bar{\lambda}_{max} &= \sum_{N=1}^{\frac{1}{2}K(K-1)} 0.5 \cdot P_K(N) \\
\bar{\zeta}_{opt} &= \sum_{N=1}^{\frac{1}{2}K(K-1)} 2[W_t + W_r + (K-1)W_s] \cdot P_K(N)
\end{aligned} \quad (13)$$

Next, we derive λ_{max} and ζ_{opt} when MIMO-NC is adopted. We still use p_1 and p_2 to denote the uplink and downlink compatibility probability, respectively. When there are N links in the system, it implies that there are N vertices in the equivalent compatibility graph G . Suppose that among N vertices in G , there are c non-isolated vertices. Similar to Eq. (8) and (9), the maximum throughput and optimal energy efficiency of MIMO-NC can be expressed as

$$\begin{aligned}
\lambda_{max} &= \frac{2N}{\frac{3}{2}c + 4(N-c)} = \left(2 - \frac{5c}{4N}\right)^{-1} \\
\zeta_{opt} &= \frac{\frac{c}{2}[5W_t + 6W_r + (3K-11)W_s] + 4(N-c)[W_t + W_r + (K-1)W_s]}{2N}
\end{aligned} \quad (14)$$

where both N and c are random variables. We use $P_N(l|N)$ to denote the conditional probability that given N vertices in G , there are l isolated vertices. Accordingly, the average maximum throughput and average optimal energy efficiency of MIMO-NC can be written as

$$\begin{aligned}
\bar{\lambda}_{max} &= \sum_{N=1}^{\frac{1}{2}K(K-1)} \sum_{c=0}^N \lambda_{max} \cdot P_N(N-c|N) P_K(N) \\
\bar{\zeta}_{opt} &= \sum_{N=1}^{\frac{1}{2}K(K-1)} \sum_{c=0}^N \zeta_{opt} \cdot P_N(N-c|N) P_K(N)
\end{aligned} \quad (15)$$

To find $P_N(l|N)$, we condition it on the number of the fully-isolated vertices in G , i.e., the number of dashed links in the system. Let F_i be the event that there are i fully-isolated vertices among a total of N vertices in G . $P_N(l|N)$ can be expressed as

$$\begin{aligned}
P_N(l|N) &= \sum_{i=0}^l P_f(i) P(L=l|F_i, N) \\
&= \sum_{i=0}^l P_f(i) P_h(l-i|N-i)
\end{aligned} \quad (16)$$

where $P_f(i)$ denotes the probability of event F_i , and $P_h(l-i|N-i)$ represents the probability that the remaining $N-i$ solid links in the system would result in $l-i$ half-isolated vertices in G . Note that it is difficult to express $P_h(l-i|N-i)$ in a unified form since it heavily depends on the distribution of the $N-i$ solid links. Alternatively, we define a probability \bar{p}_h , which represents the average probability for a solid link to

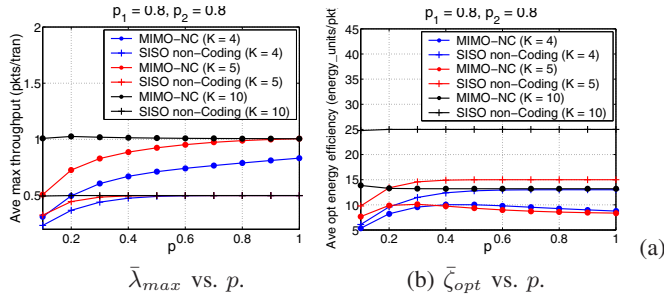


Fig. 7. $\bar{\lambda}_{max}$ and $\bar{\zeta}_{opt}$ of MIMO-NC as functions of p .

become a half-isolated vertex in G for given $N - i$ solid links in the network. Then $P_N(l|N)$ can be rewritten as

$$P_N(l|N) = \sum_{i=0}^l \binom{N}{i} \cdot (1-p_1)^i \cdot p_1^{N-i} \binom{N-i}{l-i} \cdot \bar{p}_h^{l-i} \cdot (1-\bar{p}_h)^{N-l} \quad (17)$$

Note that the reason why a solid link in the network becomes a half-isolated vertex in the equivalent compatibility graph G is that all its disjoint solid links in the system are downlink-incompatible with it. We use τ to denote the random variable representing the number of disjoint solid links of a solid link. Thus, \bar{p}_h is given by

$$\bar{p}_h = (1-p_2)^{E(\tau|N-i)} \quad (18)$$

For each solid link, $E(\tau|N-i)$ represents the average number of its disjoint solid links when there are a total of $N - i$ solid links in the system. Suppose any two links are disjoint to each other with average probability \bar{p}_d . It is clear that when a network has the complete traffic pattern, for each link, it has $\frac{1}{2}K(K-1) - 2(K-1) + 1$ disjoint links. Hence, \bar{p}_d can be approximately expressed as

$$\bar{p}_d \approx \frac{\frac{1}{2}K(K-1) - 2(K-1) + 1}{\frac{1}{2}K(K-1)} \quad (19)$$

By using \bar{p}_d , the expectation of τ with $N - i$ solid links can be given as

$$E(\tau|N-i) = \sum_{\tau=0}^{N-i} \tau \cdot \binom{N-i}{\tau} \cdot \bar{p}_d^\tau \cdot (1-\bar{p}_d)^{N-i-\tau} \quad (20)$$

Based on the above analysis, we plot $\bar{\lambda}_{max}$ and $\bar{\zeta}_{opt}$ of MIMO-NC as the functions of traffic probability p in Fig. 7. The performance of the traditional SISO and non-coding approach is also shown for comparison purpose. Traffic probability p is varied from 0.1 to 1 to represent different traffic loads. p_1 and p_2 are both set to 0.8. We can observe that MIMO-NC always surpasses the SISO and non-coding approach and such superiority becomes even more prominent as K and p increase. For example, when $K = 4$, MIMO-NC achieves 33% and 58% improvement on the average maximum throughput with respect to the SISO and non-coding approach when p is set to 0.1 and 0.8, respectively. When K increases to 5, MIMO-NC obtains 84% and 98% enhancements compared to the SISO and non-coding approach under the same settings of p . These observations are also applicable to the average optimal energy efficiency. For instance, when $K = 10$, MIMO-NC outperforms the SISO and non-coding approach by at least 45% improvement on the energy efficiency.

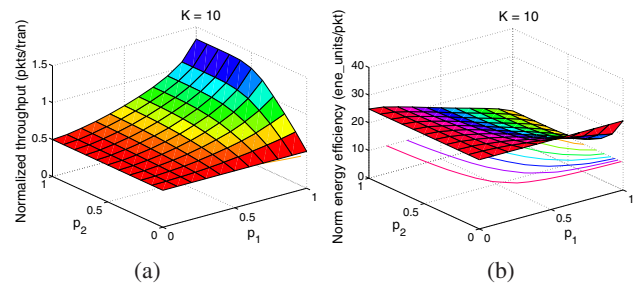


Fig. 8. Normalized throughput and energy efficiency of MIMO-NC as functions of p_1 and p_2 with circular traffic pattern among 10 users.

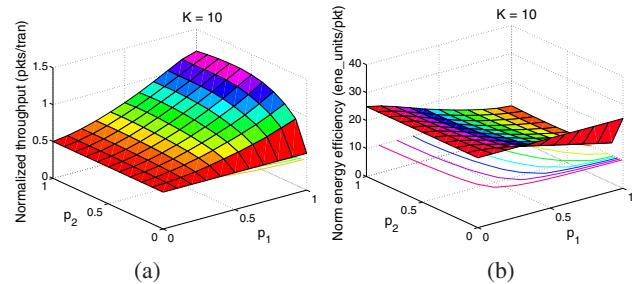


Fig. 9. Normalized throughput and energy efficiency of MIMO-NC as functions of p_1 and p_2 with full traffic pattern among 10 users.

B. Simulation Results

We have also conducted simulations to investigate various factors that affect the performance of MIMO-NC. In the simulations, K users are randomly distributed in the area. A relay node is located in the center of the area, which is one-hop away from all the users. Each packet from a user destined to another user is forwarded by the relay node. We still use p to denote the traffic probability and p_1 and p_2 to represent the uplink and downlink compatibility probability, respectively. An efficient implementation of the Edmonds' Blossom algorithm is used to find the maximum matching in the corresponding equivalent compatibility graph. Each point in the simulation curves was obtained by running on 5000 random topologies.

In the first set of simulations, we investigate the performance of MIMO-NC with circular traffic pattern. Fig. 8 shows the normalized throughput and normalized energy efficiency as functions of p_1 and p_2 when $K = 10$. From the results, we can draw some observations. First, with a higher p_1 and p_2 , better system performance is achieved. For example, the normalized throughput is 0.73 pkts/tran and the normalized energy efficiency is 17.36 energy_units/pkt when $p_1 = 0.6$ and $p_2 = 0.6$, while the normalized throughput increases to 1.07 pkts/tran and the normalized energy efficiency becomes 12.36 energy_units/pkt when $p_1 = 0.9$ and $p_2 = 0.9$. This is reasonable since the uplink and downlink compatibility probabilities directly determine the MIMO and coding opportunities. We also notice that the impact of p_2 on the system performance is less significant than that of p_1 . When p_2 becomes sufficiently large, for example, $p_2 \geq 0.5$ and $p_1 = 1$ in Fig. 8, any further increase of p_2 almost makes no difference on the system performance. Also, this threshold for p_2 to take effect on the system performance becomes higher as p_1 increases.

In the second set of simulations, the performance of a system with the full traffic pattern is investigated. In the full traffic

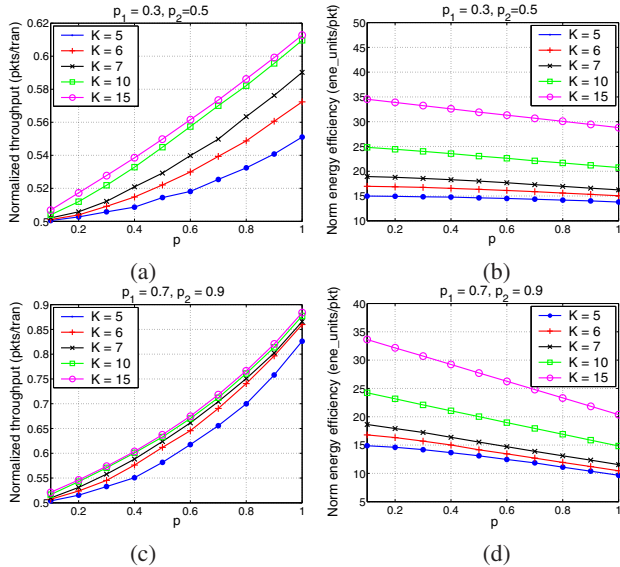


Fig. 10. Normalized throughput and energy efficiency of MIMO-NC as functions of p under different settings of p_1 and p_2 .

pattern, each user has packets to exchange with all other users, which means that there are $\frac{1}{2}K(K-1)$ links in the system. Fig. 9 shows the normalized throughput and normalized energy efficiency as functions of p_1 and p_2 when $K = 10$. Our early observations on the circular traffic pattern are also applicable here. However, the impact of the variation of p_2 on the system performance becomes even less evident. For example, when $p_2 \geq 0.3$, the normalized throughput and normalized energy efficiency almost keep constant when p_1 is fixed to 1. This result is reasonable. As the traffic becomes denser in the full traffic pattern than that in the circular traffic pattern, each link in the former case will be compatible with more other links in the downlink than that in the latter case for the same value of p_2 .

In the third set of simulations, we use traffic probability p to describe general traffic patterns, with which there is a pair of flows to be exchanged between any two users. p is varied from 0.1 to 1, which represents different traffic densities. Fig. 10 plots the normalized throughput and normalized energy efficiency of MIMO-NC as functions of p under different settings of p_1 and p_2 . We can see that the system performance is improved when p increases regardless of the values of p_1 and p_2 . For example, when $K = 10$ and p is varied from 0.1 to 1, the normalized throughput achieves 21% improvement when $p_1 = 0.3$ and $p_2 = 0.5$ (Fig. 10(a)), and 70% improvement when $p_1 = 0.7$ and $p_2 = 0.9$ (Fig. 10(c)). These results demonstrate that MIMO-NC can be better utilized when the traffic density becomes higher. It also reveals that the performance improvement with p becomes more evident under a larger p_1 and p_2 (Fig. 10(c) and (d)) than that under a smaller p_1 and p_2 (Fig. 10(a) and (b)). However, on the contrary, we can also observe that for a certain traffic density, the performance variation over K is more significant under a smaller p_1 and p_2 . This is because that the MIMO-NC gain can be fully extracted under a large p_1 and p_2 even for a small number of users.

V. CONCLUSIONS

In this paper, we have proposed a joint design of MIMO technique and network coding (MIMO-NC) to improve packet scheduling performance in wireless networks. With MIMO-NC, for the cross traffic among four users, the relay node can receive distinct packets simultaneously from two compatible users in each uplink transmission, and mix up four packets into two coded packets and concurrently transmit them in a downlink transmission. We have formalized the problem of finding an optimal schedule with MIMO-NC as a matching problem in the equivalent compatibility graph. We also studied the network performance enhanced with MIMO-NC and gave an analytical model on maximum throughput and optimal energy efficiency. Our analytical and simulation results demonstrate that by exploring coding opportunities and compatibilities among users, MIMO-NC can significantly improve the system performance.

REFERENCES

- [1] D. Tse and P. Viswanath, *Fundamentals of Wireless Communication*, Cambridge University Press, 2005.
- [2] P. Viswanath and D. Tse, "Sum capacity of the multiple antenna Gaussian broadcast channel and uplink-downlink duality," *IEEE Trans. Inf. Theory*, vol. 49, no. 8, pp. 1912-1921, Jul. 2003.
- [3] W. Yu and J. Cioffi, "Sum capacity of Gaussian vector broadcast channels," *IEEE Trans. Information Theory*, Sept. 2004.
- [4] Z. Zhang, Y. Yang and M. Zhao, "Enhancing downlink performance in wireless networks by simultaneous multiple packet transmission," *IEEE Trans. Computers*, vol. 58, no. 5, pp. 706-718, May 2009.
- [5] K. K. Wong, R. D. Murch and K. B. Letaief, "Performance enhancement of multiuser MIMO wireless communication systems," *IEEE Trans. Communications*, 2002.
- [6] R. Ahlswede, N. Cai, S. R. Li and R. W. Yeung, "Network information flow," *IEEE Trans. Information Theory*, 2000.
- [7] S. Li, R. Yeung and N. Cai, "Linear network coding," *IEEE Trans. Information Theory*, Feb. 2003.
- [8] R. Koetter and M. Medard, "An algebraic approach to network coding," *IEEE/ACM Trans. Networking*, 2003.
- [9] T. Ho, M. Medard, R. Koetter, D. R. Karger, M. Effros, J. Shi and B. Leong, "A random linear network coding approach to multicast," *IEEE Trans. Inform. Theory*, vol. 52, no. 10, October 2006.
- [10] D. S. Lun, N. Ratnakar, R. Koetter, M. Medard, E. Ahmed and H. Lee, "Achieving minimum-cost multicast: a decentralized approach based on network coding," *IEEE INFOCOM'05*, 2005.
- [11] S. Katti, H. Rahul, W. Hu, D. Katabi, M. Medard and J. Crowcroft, "XORs in the air: practical wireless network coding," *ACM SIGCOMM'06*, Pisa, Italy.
- [12] S. Sengupta, S. Rayanchu and S. Banerjee, "An analysis of wireless network coding for unicast sessions: the case for coding-aware routing," *IEEE INFOCOM'07*, 2007.
- [13] J. Liu, D. Goeckel and D. Towsley, "Bounds on the gain of network coding and broadcasting in wireless networks," *IEEE INFOCOM'07*, May 2007.
- [14] M. Ghaderi, D. Towsley and J. Kurose, "Reliability gain of network coding in lossy wireless networks," *IEEE INFOCOM'08*, 2008.
- [15] C. Fragouli, J. Widmer and J.L. Boudec, "Efficient broadcasting using network coding," *IEEE/ACM Trans. Networking*, vol. 16, no. 2, April 2008.
- [16] S. Rayanchu, S. Sen, J. Wu, S. Banerjee and S. Sengupta, "Loss-aware network coding for unicast wireless sessions: design, implementation, and performance evaluation," *ACM SIGMETRICS '08*, June 2008.
- [17] P. Chaporkar and A. Proutiere, "Adaptive network coding and scheduling for maximizing throughput in wireless networks," *ACM Mobicom'07*, September 2007.
- [18] E. Fasolo, F. Rossetto and M. Zorzi, "Network Coding meets MIMO," *NetCod*, Hong Kong, 2008.
- [19] H. N. Gabow, "An efficient implementation of Edmonds' algorithm for maximum matching on graphs," *Journal of ACM (JACM)*, vol. 23, no. 2, pp. 221-234, April 1976.
- [20] D. B. West, *Introduction to graph theory*, Prentice-Hall, 1996.